

Fast Simulation of High-Depth QAOA Circuits

Danylo Lykov^{†,‡}, Ruslan Shaydulin[†], Yue Sun[†], Yuri Alexeev[‡] and Marco Pistoia[†]

[†]Global Technology Applied Research, JPMorgan Chase, New York, NY 10017, USA

[‡]Computational Science Division, Argonne National Laboratory, Lemont, IL 60439, USA

Abstract—Until high-fidelity quantum computers with a large number of qubits become widely available, classical simulation remains a vital tool for algorithm design, tuning, and validation. We present a simulator for the Quantum Approximate Optimization Algorithm (QAOA). Our simulator is designed with the goal of reducing the computational cost of QAOA parameter optimization and supports both CPU and GPU execution. Our central observation is that the computational cost of both simulating the QAOA state and computing the QAOA objective to be optimized can be reduced by precomputing the diagonal Hamiltonian encoding the problem. We reduce the time for a typical QAOA parameter optimization by eleven times for $n = 26$ qubits compared to a state-of-the-art GPU quantum circuit simulator based on cuQuantum. Our simulator is available on GitHub: <https://github.com/jpmorganchase/QOKit>

I. INTRODUCTION

Quantum computers offer the prospect of accelerating the solution of a wide range of computational problems [1]. At the same time, only a small number of quantum algorithmic primitives with provable speedup have been identified, motivating the development of heuristics. Due to the limited availability and imperfections of near-term quantum computers, the design and validation of heuristic quantum algorithms have been largely performed in classical simulation. Additionally, classical simulators are commonly used to validate the results obtained on small-scale near-term devices. As a consequence, fast, high-performance simulators are a crucial tool for algorithm development.

Quantum Approximate Optimization Algorithm (QAOA) [2], [3] is one of the most promising quantum algorithms for combinatorial optimization. QAOA approximately solves optimization problems by preparing a parameterized quantum state such that upon measuring it, high quality solutions are obtained with high probability.

Due to the difficulty of theoretical analysis, QAOA performance is commonly analyzed numerically. Recently, Boulebnane and Montanaro demonstrated numerically that QAOA scales better than state-of-the-art classical solvers for random 8-SAT [4]. The demonstrated potential of QAOA as an algorithmic component that enables quantum speedups motivates the development of tools for its numerical study. Since QAOA performance increases with circuit depth p , it is particularly interesting to simulate high-depth QAOA. For example, Ref. [4] only observes a

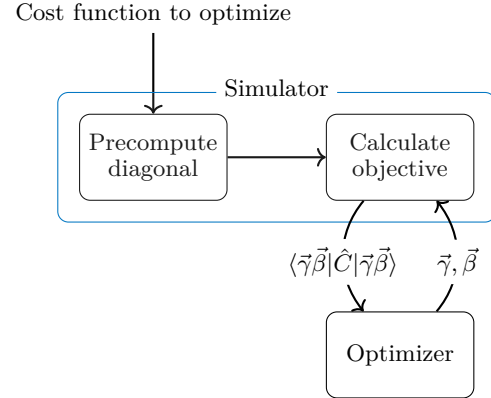


Fig. 1: Overview of the simulator. Precomputing and storing the diagonal cost operator reduces the cost of both simulating the phase operator in QAOA as well as evaluating the QAOA objective.

quantum speedup with QAOA for $p \gtrsim 14$ and Ref. [5] demonstrates that $p \geq 12$ is needed for QAOA to be competitive with classical solvers for the MaxCut problem on 3-regular graphs.

We implement a fast state-vector simulator for the study of QAOA. Our simulator is optimized for simulating QAOA with high depth as well as repeated evaluation of QAOA objective, which is required for tuning the QAOA parameters. To accelerate the simulation, we first precompute the values of the function to be optimized (see Fig. 1). The result of precomputation is reused during the parameter optimization. The precomputation algorithm is easy to parallelize, making it amenable to GPU acceleration. The precomputation requires storing an exponentially-sized vector, increasing the memory footprint of the simulation by only 12.5%. Our technique is general, and we implement transverse-field and Hamming-weight-preserving XY mixers. We achieve orders of magnitude speedups over state-of-the-art state-vector and tensor-network simulators and demonstrate scalability to 1,024 GPUs [6]. We implement the developed simulator in QOKit framework, which also provides optimized parameters and additional tooling for a set of commonly studied problems

We use the developed simulator to simulate QAOA with up to 40 qubits, enabling a scaling analysis of QAOA performance on the LABS problem. The details of the observed quantum speedup over state-of-the-art classical solvers are described in detail in Ref. [6].

II. BACKGROUND

Consider the problem of minimizing a cost function $f : \mathcal{F} \rightarrow \mathbb{R}$ defined on a subset \mathcal{F} of the Boolean cube \mathbb{B}^n . The bijection $\mathbb{B} \cong \{-1, 1\}$ is used to express the cost function f as a polynomial in terms of spins

$$f(\mathbf{s}) = \sum_{k=1}^L w_k \prod_{i \in \mathbf{t}_k} s_i, \quad s_i \in \{-1, 1\}. \quad (1)$$

The polynomial is defined by a set of terms $\mathcal{T} = \{(w_1, \mathbf{t}_1), (w_2, \mathbf{t}_2), \dots, (w_L, \mathbf{t}_L)\}$. Each term consists of a weight $w_k \in \mathbb{R}$ and a set of integers \mathbf{t}_k from 1 to n , i.e., $\mathbf{t}_k \subseteq \{i \mid 1 \leq i \leq n\}$. Constant offset is encoded using a term $(w_{\text{offset}}, \emptyset)$.

We present numerical results for QAOA applied to the following two problems. First, we consider the commonly studied MaxCut problem. The cost function for the MaxCut problem is given by $\sum_{i,j \in E} \frac{1}{2} s_i s_j - \frac{|E|}{2}$ where $G = (V, E)$ is the problem graph, $\mathcal{T} = E$, and $s_i \in \{-1, 1\}$ are the variables to be optimized. Second, we consider the Low Autocorrelation Binary Sequences (LABS) problem. The cost function for the LABS problem with n variables is given by $2 \sum_{i=1}^{n-3} s_i \sum_{t=1}^{\lfloor \frac{n-i-1}{2} \rfloor} \sum_{k=t+1}^{n-i-t} s_{i+t} s_{i+k} s_{i+k+t} + \sum_{i=1}^{n-2} s_i \sum_{k=1}^{\lfloor \frac{n-i}{2} \rfloor} s_{i+2k}$.

The QAOA state is prepared by applying phase and mixing operators in alternation. The phase operator is diagonal and adds phases to computational basis states based on the values of the cost function. The mixing operator, also known as the mixer, is non-diagonal and is used to induce non-trivial dynamics. The phase operator is created using the diagonal problem Hamiltonian given by $\hat{C} = \sum_{\mathbf{x} \in \mathcal{F}} f(\mathbf{x}) |\mathbf{x}\rangle\langle\mathbf{x}|$, where $|\mathbf{x}\rangle$ is a computational basis quantum state. The spectrum of the operator matches the values of the cost function to be optimized, thus the ground state $|\mathbf{x}^*\rangle$ of such Hamiltonian corresponds to the optimal value $f(\mathbf{x}^*)$. The goal of QAOA is to bring the quantum system close to a state such that upon measuring it, we obtain \mathbf{x}^* with high probability.

The QAOA circuit is given by

$$|\vec{\gamma}\vec{\beta}\rangle = \prod_{l=1}^p \left(e^{-i\beta_l \hat{M}} e^{-i\gamma_l \hat{C}} \right) |s\rangle.$$

If $\mathcal{F} = \mathbb{B}^n$, the standard choices are the transverse-field operator $\hat{M} = \sum_i X_i$ as the mixer and uniform superposition $|+\rangle^{\otimes n}$ as the initial state. The free parameters γ_l and β_l are chosen to minimize the expected solution quality $\langle \vec{\gamma}\vec{\beta} | \hat{C} | \vec{\gamma}\vec{\beta} \rangle$, typically using a local optimizer.

III. SIMULATION OF QAOA USING Q0Kit

The convention of representing a quantum program as a sequence of quantum gates may pose limitations when simulating QAOA classically. In standard gate-based simulators such as Qiskit and QTensor, the phase operator must be compiled into gates. The number of these gates typically scales polynomially with the number of terms

in the cost function $|\mathcal{T}|$. The overhead is especially large when considering objectives with higher order terms, such as k -SAT with $k > 3$ and Low Autocorrelations Binary Sequences (LABS) problem. Existing state-vector simulators primarily work by iterating over each gate in the circuit and modifying the state vector. By exploiting the structure of the circuit, our state-vector simulator recognizes that each application of the phase operator involves the same set of gates and that the set acts as a diagonal operator, reducing the cost of simulation.

A. Precomputation of the cost vector

Q0Kit precomputes the diagonal elements in the operator \hat{C} , which are the values of the cost function f for each assignment of the input. The values are stored as a 2^n -sized cost vector, which encodes all the information about the problem Hamiltonian. Q0Kit provides simple high-level API which supports both cost functions defined as a polynomial on spins (see Listing 1), as well as a Python lambda function. For precomputation using polynomial terms (Eq. 1), we start by allocating an array of zeroes, and iterate over terms in \mathcal{T} , applying a GPU kernel in-parallel for each element of the array. The binary representation of an index of a vector element corresponds to qubit values in a basis state. This allows us to calculate the value of the term using bitwise-XOR and "population count" operations. The kernel calculates the term value and adds it to a single element of the vector in-place. This has the advantage of locality, which is beneficial for GPU parallelization and distributed computing.

To apply the phase operator with parameter γ_l , we perform an element-wise product of the state vector and $e^{-i\gamma_l \hat{C}}$, where \vec{C} is the cost vector and the exponentiation is applied element-wise. After simulating the QAOA evolution, we reuse the precomputed \vec{C} to evaluate the expected solution quality $\langle \vec{\gamma}\vec{\beta} | \hat{C} | \vec{\gamma}\vec{\beta} \rangle$ by taking an inner product between \vec{C} and the QAOA state.

B. Mixing operator

Application of the mixing operator is more challenging than that of the phase operator, and accounts for the vast majority of computational cost in our simulation. We briefly discuss the implementation using the example of the transverse-field mixer. Other mixers are implemented similarly. The transverse-field mixer can be decomposed into products of local gates as $U_M = e^{-i\beta \sum_i X_i} = \prod_i e^{-i\beta X_i}$. Each gate $e^{-i\beta X} = \cos(\beta)I - i \sin(\beta)X$ "mixes" two probability amplitudes, and all n gates mix all 2^n probability amplitudes. Classical simulation of this operation requires all-to-all communication, where each output vector element depends on every entry of the input vector. For example, for $\beta = \pi/2$ the phase operator implements the Walsh-Hadamard transform, which is a Fourier transform on the Boolean cube \mathbb{B}^n . The definition of QAOA mixing operator via Walsh-Hadamard transform was known for a long time, see e.g., Refs. [3], [7]. In fact,

the ability of quantum computers to efficiently perform Walsh-Hadamard transform [8], [9], which is the central building block for the famed Grover’s algorithm [10], was the inspiration for the definition of the QAOA mixer [3].

Our GPU simulator implements each $e^{-i\beta x_i}$ of the mixing operator by applying a GPU kernel which modifies two elements of the state vector. Since these calculations do not interfere with each other, the updates on all pairs of elements in the state vector can be done in place and in parallel, hence well-utilizing the parallelization power of the GPU. The algorithm for simulating a single $e^{-i\beta x_i}$ is described in Algorithm 1. To simulate the full mixer, Algorithm 1 is applied to each qubit $i \in [n]$, as shown in Algorithm 2. Both algorithms modify the state vector in-place without using any additional memory.

The full QAOA simulation algorithm in QOKit is described in Algorithm 3. Furthermore, we implement the simulation using NVIDIA cuQuantum framework, by replacing Algorithm 2 with calls to the cuStateVec library. We refer to this implementation as QOKit (cuStateVec). In addition to the conventional transverse-field mixing Hamiltonian $M = \sum_i x_i$, we implement Hamming-weight-preserving XY mixer whose Hamiltonian is given by a set of two-qubit operators $M = \sum_{\langle i,j \rangle} \frac{1}{2}(x_i x_j + y_i y_j)$ for $\langle i,j \rangle$ corresponding to the edges of ring or complete graphs. The implementation leverages the observation that Algorithms 1 and 2 can be easily extended to SU(4) operators.

Algorithm 1 Fast SU(2) On A State Vector

Input: Vector $\mathbf{x} \in \mathbb{C}^N$ with $N = 2^n$, a unitary matrix $U_\star = \begin{pmatrix} a & -b^\star \\ b & a^\star \end{pmatrix} \in \text{SU}(2)$ and a positive integer $d \in [n]$

Output: Vector $\mathbf{y} = U\mathbf{x}$, where $U = \mathbb{I}^{\otimes(d-1)} \otimes U_\star \otimes \mathbb{I}^{\otimes(n-d)}$ and \mathbb{I} is the 2-dimensional identity matrix

- 1: Create a reference \mathbf{y} to input vector \mathbf{x}
 - 2: **for** $k_1 = 1$ **to** 2^{n-d} **do**
 - 3: **for** $k_2 = 1$ **to** 2^{d-1} **do**
 - 4: Compute indices:

$$l_1 \leftarrow (k_1 - 1)2^d + k_2$$

$$l_2 \leftarrow (k_1 - 1)2^d + k_2 + 2^{d-1}$$
 - 5: Simultaneously update \mathbf{y}_{l_1} and \mathbf{y}_{l_2} :

$$\mathbf{y}_{l_1} \leftarrow a\mathbf{y}_{l_1} - b^\star\mathbf{y}_{l_2}$$

$$\mathbf{y}_{l_2} \leftarrow b\mathbf{y}_{l_1} + a^\star\mathbf{y}_{l_2}$$
 - 6: **end for**
 - 7: **end for**
 - 8: **return** \mathbf{y}
-

C. Distributed simulation

A typical supercomputer consists of multiple identical compute nodes connected by a fast interconnect. Each node in turn consists of a CPU and several GPUs. Since GPUs are much faster in our simulation tasks, we do not use CPUs in our distributed simulation. Each of K GPUs holds a slice of the state vector, which corresponds

Algorithm 2 Fast Uniform SU(2) Transform (Single-node)

Input: Vector $\mathbf{x} \in \mathbb{C}^N$, a unitary matrix $U \in \text{SU}(N)$ decomposable into tensor product of n unitary matrices in SU(2), i.e. $U = \bigotimes_{i=1}^n U_i = U_n \otimes \cdots \otimes U_2 \otimes U_1$,

where $U_i = \begin{pmatrix} a_i & -b_i^\star \\ b_i & a_i^\star \end{pmatrix} \in \text{SU}(2)$ and $N = 2^n$

Output: Vector $\mathbf{y} = U\mathbf{x}$

- 1: Create a reference \mathbf{y} to input vector \mathbf{x}
 - 2: **for** $i = 1$ **to** n **do**
 - 3: Apply Algorithm 1 with $U_\star \leftarrow U_i$ and $d \leftarrow i$
 - 4: **end for**
 - 5: **return** \mathbf{y}
-

Algorithm 3 Fast Simulation of QAOA

Input: Initial vector $\mathbf{x} \in \mathbb{C}^N$, QAOA circuit parameters $\beta, \gamma \in \mathbb{R}^p$, cost function $f : \mathbb{Z}_2^n \rightarrow \mathbb{R}$, where $N = 2^n$

Output: State vector after applying the QAOA circuit to \mathbf{x}

- 1: Pre-compute (and cache) cost values for all binary strings into a vector $\mathbf{c} \in \mathbb{C}^N$
 - 2: Initialize output vector $\mathbf{y} \leftarrow \mathbf{x}$
 - 3: **for** $l = 1$ **to** p **do**
 - 4: Apply phase operator:

$$\mathbf{y}_k \leftarrow e^{-i\gamma c_k} \mathbf{y}_k$$
end for
 - 5: Apply mixing operator:

$$\text{Apply Algorithm 2 on } \mathbf{y} \text{ with } a_i \leftarrow \cos \beta_l, b_i \leftarrow \sin \beta_l \forall i \in [n]$$
 - 6: **end for**
 - 7: **return** \mathbf{y}
-

to fixing the values of a set of $k = \log_2(K)$ qubits. For example, for $K = 2$ GPUs, the first GPU holds probability amplitudes for states with the first qubit in state $|0\rangle$, while the second GPU holds states with first qubit in the state $|1\rangle$. In general, using K GPUs allows us to increase the simulation size by k qubits.

During the precomputation, the cost vector \vec{C} is sliced in the same way as the state vector. Due to the locality discussed above, the precomputation and the phase operator application do not require any communication across GPUs. The most expensive part of the simulation is the mixing operator, since it requires an all-to-all communication pattern. In our simulation we distribute the state vector by splitting it into K chunks, which corresponds to fixing first k qubits, which we call *global qubits*. Bits of the binary representation of the node index determine the fixed qubit values. The remaining $n - k$ qubits are referred to as *local qubits*.

The mixer application starts by applying the $e^{-i\beta x_i}$ gates that correspond to local qubits. To apply x rotations

on global qubits, we reshape the distributed state vector using the `MPI_Alltoall` MPI collective. This operation splits each local state vector further into K subchunks and transfers subchunk A of process B into subchunk B of process A . If each subchunk consists of one element and we arrange the full state vector in a matrix with process id as column index and subchunk id as the row index, then the call to `MPI_Alltoall` performs a transposition of this matrix. For a n -qubit simulation the algorithm requires $2k \leq n$ to ensure that there is at least one element in each subchunk. Consider the state vector reshaped as a tensor V_{abc} with a being the process id representing the k global qubits, b being a multi-index of first k local qubits, and c being a multi-index of the last $n - 2k$ qubits. Then the `MPI_Alltoall` operation corresponds to a transposition of the first two indices, i.e., $V_{abc} \rightarrow V_{bac}$. Thus, after this transposition, the global qubits become local and we are free to apply operations on those k global qubits locally in each process. The algorithm concludes by applying the `MPI_Alltoall` once again to restore the original qubit ordering. This algorithm is described in Algorithm 4.

Algorithm 4 Fast Uniform SU(2) Transform (Multi-node)

Input: Vector $\mathbf{x} \in \mathbb{C}^N$ distributed over K nodes, a unitary matrix $U = \bigotimes_{i=1}^n U_i = U_n \otimes \dots \otimes U_2 \otimes U_1$, where $U_i \in \text{SU}(2)$ and $N = 2^n$

Output: Distributed vector $\mathbf{y} = U\mathbf{x}$

- 1: Create a reference \mathbf{y} to the local slice of input vector \mathbf{x}
 - 2: **for** $i = 1$ **to** $n - \log_2 K$ **do**
 - 3: Apply Algorithm 1 with $U_\star \leftarrow U_i$ and $d \leftarrow i$ to the local slice \mathbf{y} .
 - 4: **end for**
 - 5: Run in-place `MPI_AlltoAll` on the local slice \mathbf{y} .
 - 6: **for** $i = n - \log_2 K + 1$ **to** n **do**
 - 7: Apply Algorithm 1 with $U_\star \leftarrow U_i$ and $d \leftarrow i - \log_2 K$ to the local slice \mathbf{y} .
 - 8: **end for**
 - 9: Run in-place `MPI_AlltoAll` on the local slice \mathbf{y} .
 - 10: **return** \mathbf{y}
-

The `MPI_Alltoall` is known to be a challenging collective communication routine, since it requires the total transfer of the full state vector K times. There exist many algorithms for this implementation [11], [12], each with its own trade-offs. Furthermore, the same communication problem occurs in applying distributed Fast Fourier Transform (FFT), which has been studied extensively [13], [14], [15], [16]. In this work, we use the out-of-the-box MPI implementation Cray MPICH. Utilizing the research on distributed FFT may help further improve our implementation.

IV. EXAMPLES OF USE

QOKit consists of two conceptual parts:

- 1) Low-level simulation API defined by an abstract class `qokit.fur.QAOAFastSimulatorBase`
- 2) Easy-to-use one-line methods for simulating MaxCut, LABS and portfolio optimization problems

The low-level simulation API is designed to provide more flexibility in terms of inputs, methods and outputs of simulation. The simulation inputs can be specified by providing either terms \mathcal{T} or existing pre-computed diagonal vector. The simulation method is specified by using a particular subclass of `qokit.fur.QAOAFastSimulatorBase` or by using a shorthand method `qokit.fur.choose_simulator`. This simulator class is the main means of simulation, with input parameters being passed in the constructor, the simulation done in `simulate_qaoa` method, and outputs type specified by choosing a corresponding method of the simulator object. An example of using the simulator with input terms parameter is shown in Listing 1.

```

1 import qokit
2 simclass = qokit.fur.choose_simulator(name='auto')
3 n = 28 # number of qubits
4 # terms for all-to-all MaxCut with weight 0.3
5 terms = [(i, j) for i in range(n) for j in
           range(i+1, n)]
6 sim = simclass(n, terms=terms)
7 # get precomputed cost vector
8 costs = sim.get_cost_diagonal()
9 result = sim.simulate_qaoa(gamma, beta)
10 E = sim.get_expectation(result)

```

Listing 1: Evaluating the QAOA objective for weighted MaxCut problem on an all-to-all graph using QOKit.

QOKit implements five different simulator classes that share the same API:

- 1) `python` – A portable CPU `numpy`-based version
- 2) `c` – Custom CPU simulator implemented in C
- 3) `nbcuda` – GPU simulator using `numba`
- 4) `gpumpi` – A distributed version of the GPU simulator
- 5) `cusvmpi` – A distributed GPU simulator with `cuSateVec` as backend

To choose from the simulators, one may use one of the following three methods, depending on the choice of mixer type:

- 1) `qokit.fur.choose_simulator()`
- 2) `qokit.fur.choose_simulator_xyring()`
- 3) `qokit.fur.choose_simulator_xycomplete()`

Each of these simulators accepts an optional `name` parameter. The default simulator is chosen based on existence of GPU or configured MPI environment. An example of using a custom mixer for simulation is provided in Listing 2.

```

1 import qokit
2 simclass = qokit.fur.choose_simulator_xycomplete()
3 n = 40
4 terms = qokit.labs.get_terms(n)
5 sim = simclass(n, terms=terms)
6 result = sim.simulate_qaoa(gamma, beta)
7 E = sim.get_expectation(result)

```

Listing 2: Using QOKit with a different mixing operator:

$M = \sum_{\langle i,j \rangle} \frac{1}{2}(X_i X_j + Y_i Y_j)$ for tuples $\langle i, j \rangle$ from a complete graph on qubits.

The constructor of each simulator class accepts one of `terms` or `costs` argument. The `terms` argument is a list of tuples (w_k, \mathbf{t}_k) , where w_k is the weight of product defined by \mathbf{t}_k , which is a tuple of integers specifying the indices of Boolean variables involved in this product, as described in Equation 1. The simulation method returns a `result` object, which is a representation of the evolved state vector. The data type of this object may change depending on simulator type, and for best portability it is advised to use the output methods instead of directly interacting with this object. The output methods all have `get_` prefix, accept the `result` object as their first argument, and return CPU values. These methods are:

- 1) `get_expectation(result)`
- 2) `get_overlap(result)`
- 3) `get_statevector(result)`
- 4) `get_probabilities(result)`

When evaluating the expectation and overlap with the ground state, the cost vector from the phase operator is used by default. This vector is precomputed at the class instantiation and can be retrieved using `get_cost_diagonal()` method. Alternatively, the user may specify a custom cost vector by passing it as the `costs` argument when calling `get_expectation` or `get_overlap`.

The output methods may accept additional optional arguments depending on the type of the simulator. For example, GPU simulators’ `get_probabilities` method has `preserve_state` argument (default `True`) which specifies whether to preserve the statevector for additional calculations; otherwise, the norm-square operation will be applied in-place. In both cases, the method returns a real-valued array of probabilities. Distributed GPU simulators accept `mpi_gather` argument (default `True`) that signals the method to return a full state vector on each node. Specifying `mpi_gather = True` guarantees that the same code will produce the same result if the hardware-specific simulator class is changed. An example of using QOKit for distributed simulation is provided in Listing 3.

```

1 import qokit
2 simclass = qokit.fur.choose_simulator(name='
   cusvmpi')
3 n = 40
4 terms = qokit.labs.get_terms(n)
5 sim = simclass(n, terms=terms)
6 result = sim.simulate_qaoa(gamma, beta)
7 E = sim.get_expectation(result, preserve_state=
   False)

```

Listing 3: Evaluating the QAOA objective for LABS problem using MPI on a distributed computing system using QOKit. The `preserve_state` argument is used to reduce memory usage when evaluating the expectation value.

V. PERFORMANCE OF QOKit

We now present a comparison of QOKit performance to state-of-the-art state-vector and tensor-network quantum simulators. We show that our framework has lower run-times and scales well to large supercomputing systems. All reported benchmarks are executed on the Polaris supercomputer accessed through the Argonne Leadership Computing Facility. Single-node results are obtained using a compute node with two AMD EPYC 7713 64-Core CPUs with 2 threads per core, 503 GB of RAM and an NVIDIA A100 GPU with 80 GB of memory. In all experiments the state vector is stored with double precision (`complex128` data type).

A. CPU and GPU simulation

The CPU simulation is implemented in two ways: using the NumPy Python library and using a custom C code (“c” simulator above). The latter is more performance, so we only report the results with c simulator. We evaluate the CPU performance by simulating QAOA with $p = 6$ on MaxCut random regular graphs.

Figure 2 shows a comparison of runtime for varying number of qubits for commonly-used CPU simulators. We use QOKit c simulator, Qiskit Aer state-vector simulator version 0.12.2, and OpenQAOA “vectorized” simulator version 0.1.3. We observe $\approx 5 - 10\times$ speedup against Qiskit [17] and OpenQAOA [18] across a wide range of values of n . We note that the simulation method in QAOAKit [19] is Qiskit, which is why we do not benchmark it separately.

We evaluate the GPU performance by evaluating time to simulate one layer of QAOA applied to the LABS problem. Fig. 3 provides a comparison between QOKit and commonly used state-vector (Qiskit [17] version 0.43.3, `cuStateVec` [20]) and tensor-network (`cuTensorNet` [20], `QTensor` [21]) simulators. We used CuQuantum Python package version 23.6.0 and `cuda toolkit` version 14.4.4. The tensor network timing is obtained by running calculation of a single probability amplitude for various values of

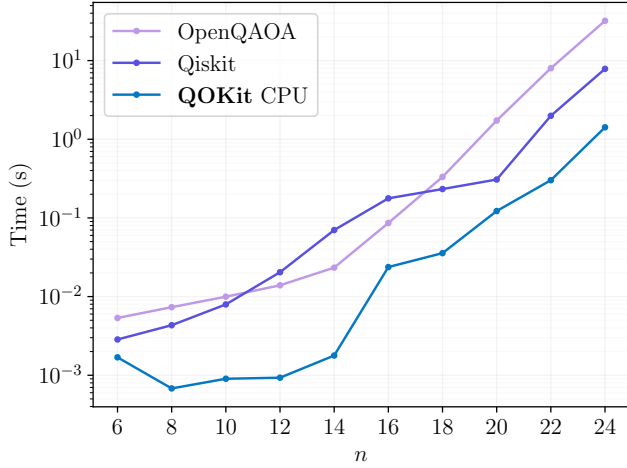


Fig. 2: Runtime of end-to-end simulation of QAOA expectation value with $p = 6$ on MaxCut problem on 3-regular graphs with commonly-used CPU simulators for QAOA. Their time plotted is the mean over 5 runs.

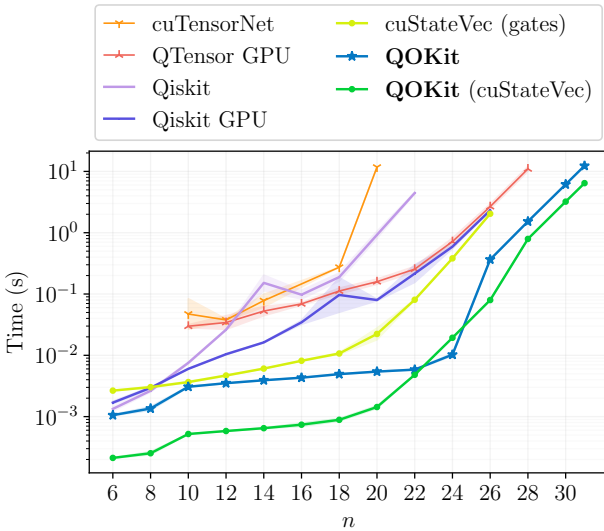


Fig. 3: Time to apply a single layer of QAOA for the LABS problem with commonly-used CPU and GPU simulators. QOKit simulator uses the precomputation which is not included in current plot. The precomputation time is amortized, as shown on Figure 4. QOKit can be configured to use cuStateVec for application of the mixing operator, which provides the best results.

$1 \leq p \leq 15$ and dividing the total contraction time by p . Deep circuits have optimal contraction order that produces contraction width equal to n . Since obtaining batches of amplitudes does not produce high overhead [22], this serves as a lower bound for full state evolution. Note that the so-called “lightcone approach”, wherein only the reverse causal cone of the desired observable is simulated, does not significantly reduce the resource requirements due

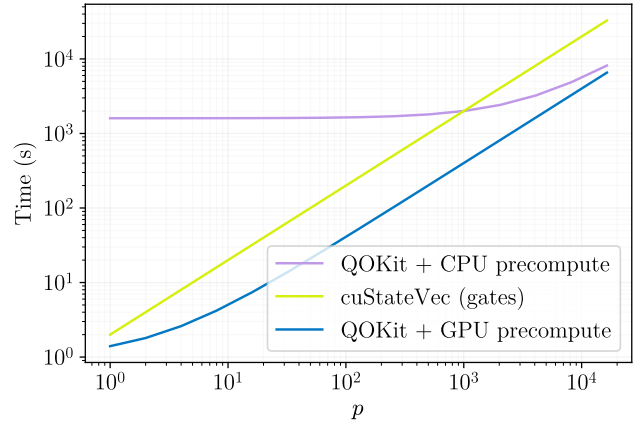


Fig. 4: Total simulation time vs. number of layers in QAOA circuit for LABS problem with $n = 26$. The GPU precomputation is fast enough to provide speedup over the gate-based state-vector simulation (cuStateVec) even for a single evaluation of the QAOA circuit.

to the high depth and connectivity of the phase operator. For QTensor, “tamaki_30” contraction optimization algorithm is used. CuTensorNet contraction is optimized with default settings. It is possible that the performance can be improved by using diagonal gates [23], which are only partially supported by cuTensorNet at this moment.

For $n > 20$, we observe that the precomputation provides orders of magnitude speedups for simulation of a QAOA layer. The LABS problem has a large number of terms in the cost function, leading to deep circuits which put tensor network simulators at a disadvantage. As a consequence, we observe that tensor network simulators are slower than state-vector simulation. We also observe that using cuStateVec as a backend for mixer gate simulation provides additional $\approx 2\times$ speedup, possibly due to higher numerical efficiency achieved by in-house NVIDIA implementation. We do not include the precomputation cost in Fig. 3. This cost is amortized over application of a QAOA layer as shown in Fig. 4, and is negligible if precomputation is performed on GPU. Simulation of each layer in a deep quantum circuit has the same time and memory cost. Thus, to obtain the time for multiple function evaluations, one can simply use this plot with aggregate number of layers in all function evaluations.

Our best GPU performance for QAOA on LABS problem is ≈ 6 seconds per QAOA layer for $n = 31$ using double precision. This simulation requires the same memory amount as one with $n = 32$ using single precision. In addition to our own implementation, we benchmark the same simulator as in the Ref. [24] on the LABS problem. For smaller $n \leq 26$, QOKit with cuStateVec shows a $\approx 20\times$ speedup from our precomputation approach. We discuss the choice of cuStateVec as the baseline as well as other state-of-the-art simulation techniques in Sec. VI.

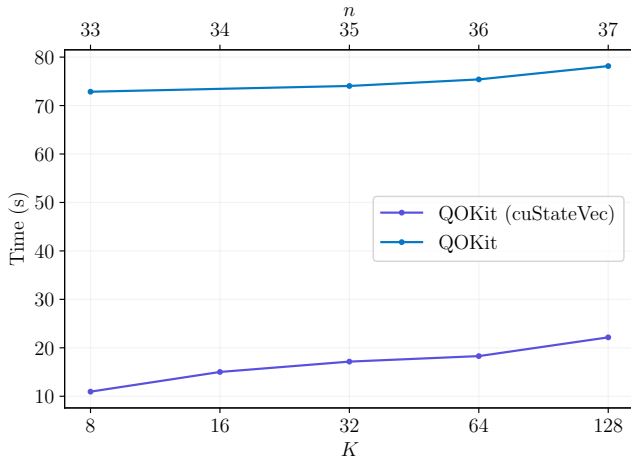


Fig. 5: Weak scaling results for simulation of 1 layer of LABS QAOA on Polaris supercomputer. We observe that cuStateVec backend has lower communication overhead, leading to lower overall runtime.

B. Distributed simulation

Finally, we scale the QAOA simulation to $n = 40$ qubits using 1024 GPUs of the Polaris supercomputer. At $n = 40$, we observe a runtime of ≈ 20 s per layer. The results of the simulation are discussed in detail in Ref. [6]. Here, we focus on the technical aspects of the simulation.

In distributed experiments, we use compute nodes of Polaris with 4 NVIDIA A100 GPUs with 40GB of memory. The maximum values of f are known for $n < 65$, and they are less than 2^{16} . Therefore, we are able to store the precomputed diagonal as a 2^n vector of uint16 values, which reduces the memory overhead of the cost value vector. As discussed in Section III-C, the most expensive part of this simulation is communication. We implement two approaches for this simulation, a custom MPI code that uses MPI_Alltoall collective and an implementation leveraging the distributed index swap operation in cuStateVec. Weak scaling results in Figure 5 demonstrate the advantage of cuStateVec implementation of communication. The GPUs co-located on a single node are connected with high-bandwidth NVLink network. To transfer data between nodes, GPU data need to transfer to CPU for subsequent transfer to another node. This requires the communication to correctly choose the communication method depending on GPU location. MPI has built-in support which can be enabled using MPI_GPU_SUPPORT_ENABLED environment variable. However, it shows worse performance than the cuStateVec communication code, which uses direct CUDA peer-to-peer communication calls for local GPU communication. We observe that our performance is comparable to distributed simulation reported in Ref. [24], despite having $2\times$ fewer GPUs per node. This is due to the majority of time being spent in communication, which is confirmed by

our smaller-scale profiling experiments. Further research, including adapting the communication patterns used in high-efficiency FFT algorithms, may improve our results.

VI. RELATED WORK

Classical simulation of quantum systems is a dynamic field with a plethora of simulation algorithms [25], [21], [26], [27] and a variety of use cases [28], [29]. The main approaches to simulation are tensor network contraction algorithms and state-vector evolution algorithms. Tensor network algorithms are able to utilize the structure of quantum circuit and need not store the full 2^n -dimensional state vector when simulating n qubits. Instead, they construct a tensor network and contract it in the most efficient way possible. This approach works best when the circuit is shallow, since the tensor network contraction can be performed across qubit dimension instead of over time dimension. The main research areas of this approach are finding the best contraction order [30], [31], [32] and applying approximate simulation algorithms [33], [34]. However, while there is no theoretical limitation on simulating deep circuits using tensor networks, it is challenging to implement a performant simulator of deep quantum circuits based on tensor networks, as demonstrated by the numerical experiments above.

The state vector evolution algorithms are more straightforward and intuitive to implement. The main limitation of state-vector simulator is the 2^n size of the state vector. There are many approaches to improve state-vector simulators. Compressing the state vector has been proposed to reduce the memory requirement and enable the simulation of a higher number of qubits [35]. To utilize the structure in the set of quantum gates, some state-vector simulators use the gate fusion approach [36], [37], [38], [39]. The idea is to group the gates that act on a set of F qubits, then create a single F -qubit gate by multiplying these gates together. This approach is often applied for $F = 2$ and provides significant speed improvements. Computing the fused gate requires storing 4^F complex numbers, which is a key limitation. Our approach corresponds to using gate fusion with $F = n$, but the group of gates is known to produce a diagonal gate, which can be stored as a vector of only 2^n elements.

In our comparison in Sec. V-A, we do not enable gate fusion in cuStateVec. While gate fusion may improve the performance of cuStateVec, we believe it is very unlikely to achieve the same efficiency as our method of using the precomputed diagonal cost operator. Our argument is based on examining the results reported in Ref. [24]. The central challenge for gate fusion is presented by the fact that the phase operator for the LABS problem requires many gates to implement. For example, for $n = 31$, the LABS cost function has $\approx 75n$ terms, with many of them being 4-order terms. If decomposed into 2-qubit gates, the circuit for QAOA with $p = 1$ for the LABS problem has $\approx 160n$ gates after compilation. For comparison, QAOA

circuit from Ref. [24] for $n = 33$ and $p = 2$ has $50n$ un-fused gates, which is $\approx 7\times$ fewer. After gate fusion, the circuits from Ref. [24] have $\approx 4n$ fused gates. Our precomputation approach reduces the number of gates to practically only the n mixer gates. Thus, assuming that application of a single gate takes the same amount of time for any statevector simulator, we can expect a speedup in the range of $4 - 160\times$. We note that while this estimate does not take into account various other time factors and variation in gate application times, it provides intuition for why we rule out gate fusion outperforming our techniques.

While there exist a multitude of quantum simulation frameworks, the best results for state-vector GPU simulation that we found in the literature were reported in Ref. [24] (cuQuantum) and Ref. [36] (qsim). Ref. [24] reports ≈ 10 seconds for simulating QAOA with $p = 2$, $n = 33$ qubits and 1650 gates, using the `complex64` data type on a single A100 GPU with 80 GB memory. Ref. [36] presents single-precision simulation results on a A100 GPU with 40 GB memory. The benchmark uses random circuits of depth of 20. The reported simulation time for $n = 32$ is ≈ 6 seconds. Notably, this time may depend significantly on the structure of the circuit since it impacts the gate fusion, as shown in Ref. [37]. Assuming similar gate count, these results show very similar performance, since the simulation in Ref. [24] is two times larger. This motivates our use of cuQuantum (Ref. [24]) as a baseline state-of-the-art state-vector quantum simulator.

Symmetry of the function to be optimized has been shown to enable a reduction in the computational and memory cost of QAOA simulation [40], [41], [42]. While we do not implement symmetry-based optimizations in this work, they can be combined with our techniques to further improve performance.

In addition to the simulation method, many simulators differ in the scope of the project. Some simulators like cuQuantum [24] position themselves as a simulator-development SDK, with flexible but complicated API. On the other hand, there exist simulation libraries that focus on the quantum side and delegate the concern of low-level performance to other libraries [18], [19]. Many software packages exist somewhere in the middle, featuring full support for quantum circuit simulation and focusing on end-to-end optimization efforts on a particular quantum algorithm or circuit type [29], [33]. QOKit is positioned as one of such packages, as it provides both an optimized low-level QAOA-specific simulation algorithm as well as high-level quantum optimization API for specific optimization problems.

VII. CONCLUSION

We develop a fast and easy-to-use simulation framework for quantum optimization. We apply a simple but powerful optimization by precomputing the values of the cost function. We use the precomputed values to apply the QAOA phase operator by a single elementwise multiplication and

to compute the QAOA objective by a single inner product. We provide an easy-to-use high-level API for a range of commonly considered problems, as well as low-level API for extending our code to other problems. We demonstrate orders of magnitude gains in performance compared to commonly used quantum simulators. By scaling our simulator to 1,024 GPUs and 40 qubits, we enabled an analysis of QAOA on the Low Autocorrelation Binary Sequences problem that demonstrated a quantum speedup over state-of-the-art classical solvers [6].

VIII. ACKNOWLEDGEMENTS

The authors thank Tianyi Hao, Zichang He and Minzhao Liu for their invaluable feedback, technical advice and contributions to the QOKit package. The authors thank Alexander Buts and Terence Moore for their support in packaging and releasing QOKit. The authors thank their colleagues at the Global Technology Applied Research center of JPMorgan Chase for support and helpful discussions. This work used in part the resources of the Argonne Leadership Computing Facility, which is a Department of Energy Office of Science User Facility supported under Contract DE-AC02-06CH11357. The views, opinions and/or findings expressed are those of the authors and should not be interpreted as representing the official views or policies of the Department of Energy or the U.S. Government.

REFERENCES

- [1] M. A. Nielsen and I. Chuang, *Quantum computation and quantum information*, 2002.
- [2] E. Farhi, J. Goldstone, and S. Gutmann, “A quantum approximate optimization algorithm,” *arXiv:1411.4028*, 2014. [Online]. Available: 1411.4028
- [3] T. Hogg, “Quantum search heuristics,” *Physical Review A*, vol. 61, no. 5, Apr. 2000. 10.1103/physreva.61.052311. [Online]. Available: <https://doi.org/10.1103/physreva.61.052311>
- [4] S. Boulebnane and A. Montanaro, “Solving Boolean satisfiability problems with the quantum approximate optimization algorithm,” *arXiv:2208.06909*, 2022. [Online]. Available: 2208.06909
- [5] D. Lykov, J. Wurtz, C. Poole, M. Saffman, T. Noel, and Y. Alexeev, “Sampling frequency thresholds for the quantum advantage of the quantum approximate optimization algorithm,” *npj Quantum Information*, vol. 9, no. 1, Jul. 2023. 10.1038/s41534-023-00718-4. [Online]. Available: <https://doi.org/10.1038/s41534-023-00718-4>
- [6] R. Shaydulin, C. Li, S. Chakrabarti, M. DeCross, D. Herman, N. Kumar, J. Larson, D. Lykov, P. Minssen, Y. Sun, Y. Alexeev, J. M. Dreiling, J. P. Gaebler, T. M. Gatterman, J. A. Gerber, K. Gilmore, D. Gresh, N. Hewitt, C. V. Horst, S. Hu, J. Johansen, M. Matheny, T. Mengle, M. Mills, S. A. Moses, B. Neyenhuis, P. Siegfried, R. Yalovetzky, and M. Pistoia, “Evidence of scaling advantage for the quantum approximate optimization algorithm on a classically intractable problem,” *arXiv:2308.02342*, 2023. [Online]. Available: 2308.02342
- [7] A. Fabrikant and T. Hogg, “Graph coloring with quantum heuristics,” in *Proceedings of the Eighteenth National Conference on Artificial Intelligence and Fourteenth Conference on Innovative Applications of Artificial Intelligence*, R. Dechter, M. J. Kearns, and R. S. Sutton, Eds. AAAI Press / The MIT Press, 2002, pp. 22–27.

- [8] G. Brassard, P. Hoyer, and A. Tapp, “Quantum counting,” in *Automata, Languages and Programming*. Springer Berlin Heidelberg, 1998, pp. 820–831. [Online]. Available: <https://doi.org/10.1007/bfb0055105>
- [9] T. Hogg, C. Mochon, W. Polak, and E. Rieffel, “Tools for quantum algorithms,” *International Journal of Modern Physics C*, vol. 10, no. 07, pp. 1347–1361, Oct. 1999. 10.1142/s0129183199001108. [Online]. Available: <https://doi.org/10.1142/s0129183199001108>
- [10] L. K. Grover, “Quantum mechanics helps in searching for a needle in a haystack,” *Physical Review Letters*, vol. 79, no. 2, pp. 325–328, Jul. 1997. 10.1103/physrevlett.79.325. [Online]. Available: <https://doi.org/10.1103/physrevlett.79.325>
- [11] N. Nettekville, K. Fan, S. Kumar, and T. Gilray, “A visual guide to MPI all-to-all,” in *2022 IEEE 29th International Conference on High Performance Computing, Data and Analytics Workshop (HiPCW)*. IEEE, Dec. 2022. 10.1109/hipcw57629.2022.00008. [Online]. Available: <https://doi.org/10.1109/hipcw57629.2022.00008>
- [12] J. Pjesivac-Grbovic, T. Angskun, G. Bosilca, G. Fagg, E. Gabriel, and J. Dongarra, “Performance analysis of MPI collective operations,” in *19th IEEE International Parallel and Distributed Processing Symposium*. IEEE, 10.1109/ipdps.2005.335. [Online]. Available: <https://doi.org/10.1109/ipdps.2005.335>
- [13] A. Ayala, S. Tomov, A. Haidar, and J. Dongarra, “heFFTe: Highly efficient FFT for exascale,” in *Lecture Notes in Computer Science*. Springer International Publishing, 2020, pp. 262–275. [Online]. Available: https://doi.org/10.1007/978-3-030-50371-0_19
- [14] A. Gholami, J. Hill, D. Malhotra, and G. Biros, “AccFFT: A library for distributed-memory FFT on CPU and GPU architectures,” *arXiv:1506.07933*, 2016. [Online]. Available: 1506.07933
- [15] A. Ayala, S. Tomov, M. Stoyanov, A. Haidar, and J. Dongarra, “Accelerating multi - process communication for parallel 3-d FFT,” in *2021 Workshop on Exascale MPI (ExaMPI)*. IEEE, Nov. 2021. 10.1109/exampi54564.2021.00011. [Online]. Available: <https://doi.org/10.1109/exampi54564.2021.00011>
- [16] A. Ayala, S. Tomov, P. Luszczek, S. Cayrols, G. Ragghianti, and J. Dongarra, “Interim report on benchmarking FFT libraries on high performance systems” [Online]. Available: <https://icl.utk.edu/publications/interim-report-benchmarking-fft-libraries-high-performance-systems>
- [17] Qiskit contributors, “Qiskit: An open-source framework for quantum computing,” 2023.
- [18] V. Sharma, N. S. B. Saharan, S.-H. Chiew, E. I. R. Chiacchio, L. Disilvestro, T. F. Demarie, and E. Munro, “OpenQAOA – an SDK for QAOA,” *arXiv:2210.08695*, 2022. [Online]. Available: 2210.08695
- [19] R. Shaydulin, K. Marwaha, J. Wurtz, and P. C. Lotshaw, “QAOAKit: A toolkit for reproducible study, application, and verification of the QAOA,” in *2021 IEEE/ACM Second International Workshop on Quantum Computing Software (QCS)*. IEEE, Nov. 2021. 10.1109/qcs54837.2021.00011. [Online]. Available: <https://doi.org/10.1109/qcs54837.2021.00011>
- [20] “cuQuantum SDK,” <https://developer.nvidia.com/cuquantum-sdk>, accessed: 2023-07-20.
- [21] “QTensor simulator on GitHub,” <https://github.com/danlkv/QTensor>, accessed: 2023-07-20.
- [22] R. Schutski, D. Lykov, and I. Oseledets, “Adaptive algorithm for quantum circuit simulation,” *Phys. Rev. A*, vol. 101, p. 042335, Apr 2020. 10.1103/PhysRevA.101.042335. [Online]. Available: <https://link.aps.org/doi/10.1103/PhysRevA.101.042335>
- [23] D. Lykov and Y. Alexeev, “Importance of diagonal gates in tensor network simulations,” in *2021 IEEE Computer Society Annual Symposium on VLSI (ISVLSI)*, 2021. 10.1109/ISVLSI51109.2021.00088 pp. 447–452. [Online]. Available: <https://doi.org/10.1109/ISVLSI51109.2021.00088>
- [24] H. Bayraktar, A. Charara, D. Clark, S. Cohen, T. Costa, Y.-L. L. Fang, Y. Gao, J. Guan, J. Gunnels, A. Haidar, A. Hehn, M. Hohnerbach, M. Jones, T. Lubowe, D. Lyakh, S. Morino, P. Springer, S. Stanwyck, I. Terentyev, S. Varadhan, J. Wong, and T. Yamaguchi, “cuQuantum SDK: A high-performance library for accelerating quantum science,” *arXiv:2308.01999*, 2023. [Online]. Available: 2308.01999
- [25] Z. A. E. M. Dahi, E. Alba, R. Gil-Merino, F. Chicano, and G. Luque, “A survey on quantum computer simulators,” 2023. [Online]. Available: <https://api.semanticscholar.org/CorpusID:259257304>
- [26] J. Gray and S. Kourtis, “Hyper-optimized tensor network contraction,” *Quantum*, vol. 5, p. 410, mar 2021. 10.22331/q-2021-03-15-410. [Online]. Available: <https://doi.org/10.22331/q-2021-03-15-410>
- [27] A. Zulehner and R. Wille, “Advanced simulation of quantum computations,” *IEEE Transactions on Computer-Aided Design of Integrated Circuits and Systems*, vol. 38, no. 5, pp. 848–859, May 2019. 10.1109/tcad.2018.2834427. [Online]. Available: <https://doi.org/10.1109/tcad.2018.2834427>
- [28] L. Burgholzer and R. Wille, “Advanced equivalence checking for quantum circuits,” *IEEE Transactions on Computer-Aided Design of Integrated Circuits and Systems*, vol. 40, no. 9, pp. 1810–1824, Sep. 2021. 10.1109/tcad.2020.3032630. [Online]. Available: <https://doi.org/10.1109/tcad.2020.3032630>
- [29] D. Lykov, R. Schutski, A. Galda, V. Vinokur, and Y. Alexeev, “Tensor network quantum simulator with step-dependent parallelization,” in *2022 IEEE International Conference on Quantum Computing and Engineering (QCE)*. IEEE, Sep. 2022. 10.1109/qce53715.2022.00081. [Online]. Available: <https://doi.org/10.1109/qce53715.2022.00081>
- [30] C. Ibrahim, D. Lykov, Z. He, Y. Alexeev, and I. Safro, “Constructing optimal contraction trees for tensor network quantum circuit simulation,” in *2022 IEEE High Performance Extreme Computing Conference (HPEC)*. IEEE, Sep. 2022. 10.1109/hpec55821.2022.9926353. [Online]. Available: <https://doi.org/10.1109/hpec55821.2022.9926353>
- [31] T. Khakhulin, R. Schutski, and I. Oseledets, “Learning elimination ordering for tree decomposition problem,” in *Learning Meets Combinatorial Algorithms at NeurIPS2020*, 2020. [Online]. Available: <https://openreview.net/forum?id=aZ7wAnYs9v1>
- [32] E. Meiron, H. Maron, S. Mannor, and G. Chechik, “Optimizing tensor network contraction using reinforcement learning,” in *International Conference on Machine Learning*. PMLR, 2022, pp. 15 278–15 292.
- [33] J. Gray and S. Kourtis, “Hyper-optimized tensor network contraction,” p. 410, Mar. 2021. [Online]. Available: <https://doi.org/10.22331/q-2021-03-15-410>
- [34] F. Pan, P. Zhou, S. Li, and P. Zhang, “Contracting arbitrary tensor networks: General approximate algorithm and applications in graphical models and quantum circuit simulations,” *Phys. Rev. Lett.*, vol. 125, p. 060503, Aug 2020. 10.1103/PhysRevLett.125.060503. [Online]. Available: <https://link.aps.org/doi/10.1103/PhysRevLett.125.060503>
- [35] X.-C. Wu, S. Di, E. M. Dasgupta, F. Cappello, H. Finkel, Y. Alexeev, and F. T. Chong, “Full-state quantum circuit simulation by using data compression,” in *Proceedings of the International Conference for High Performance Computing, Networking, Storage and Analysis*, ser. SC ’19, 2019. 10.1145/3295500.3356155. [Online]. Available: <https://doi.org/10.1145/3295500.3356155>
- [36] S. V. Isakov, D. Kafri, O. Martin, C. V. Heidweiller, W. Mruzckiewicz, M. P. Harrigan, N. C. Rubin, R. Thomson, M. Broughton, K. Kissell, E. Peters, E. Gustafson, A. C. Y. Li, H. Lamm, G. Perdue, A. K. Ho, D. Strain, and S. Boixo, “Simulations of quantum circuits with approximate noise using qsim and Cirq,” *arXiv:2111.02396*, 2021. [Online]. Available: 2111.02396
- [37] M. Broughton, G. Verdon, T. McCourt, A. J. Martinez, J. H. Yoo, S. V. Isakov, P. Massey, R. Halavati, M. Y. Niu, A. Zlokapa, E. Peters, O. Lockwood, A. Skolik, S. Jerbi, V. Dunjko, M. Leib, M. Streif, D. Von Dollen, H. Chen, S. Cao, R. Wiersema, H.-Y. Huang, J. R. McClean, R. Babbush, S. Boixo, D. Bacon, A. K. Ho, H. Neven, and M. Mohseni, “Tensorflow quantum: A software framework for quantum machine learning,” *arXiv:2003.02989*, 2020. [Online]. Available: 2003.02989

- [38] S. Efthymiou, M. Lazzarin, A. Pasquale, and S. Carrazza, “Quantum simulation with just-in-time compilation,” *Quantum*, vol. 6, p. 814, Sep. 2022. 10.22331/q-2022-09-22-814. [Online]. Available: <https://doi.org/10.22331/q-2022-09-22-814>
- [39] M. Smelyanskiy, N. P. D. Sawaya, and A. Aspuru-Guzik, “qHiPSTER: The quantum high performance software testing environment,” *arXiv:1601.07195*, 2016. [Online]. Available: 1601.07195
- [40] R. Shaydulin, S. Hadfield, T. Hogg, and I. Safro, “Classical symmetries and the quantum approximate optimization algorithm,” *Quantum Information Processing*, vol. 20, no. 11, Oct. 2021. 10.1007/s11128-021-03298-4. [Online]. Available: <https://doi.org/10.1007/s11128-021-03298-4>
- [41] R. Shaydulin and S. M. Wild, “Exploiting symmetry reduces the cost of training QAOA,” *IEEE Transactions on Quantum Engineering*, vol. 2, pp. 1–9, 2021. 10.1109/tqe.2021.3066275. [Online]. Available: <https://doi.org/10.1109/tqe.2021.3066275>
- [42] J. Sud, S. Hadfield, E. Rieffel, N. Tubman, and T. Hogg, “A parameter setting heuristic for the quantum alternating operator ansatz,” *arXiv:2211.09270*, 2022. [Online]. Available: 2211.09270

DISCLAIMER

This paper was prepared for informational purposes with contributions from the Global Technology Applied Research center of JPMorgan Chase & Co. This paper is not a product of the Research Department of JPMorgan Chase & Co. or its affiliates. Neither JPMorgan Chase & Co. nor any of its affiliates makes any explicit or implied representation or warranty and none of them accept any liability in connection with this position paper, including, without limitation, with respect to the completeness, accuracy, or reliability of the information contained herein and the potential legal, compliance, tax, or accounting effects thereof. This document is not intended as investment research or investment advice, or as a recommendation, offer, or solicitation for the purchase or sale of any security, financial instrument, financial product or service, or to be used in any way for evaluating the merits of participating in any transaction.

The submitted manuscript includes contributions from UChicago Argonne, LLC, Operator of Argonne National Laboratory (“Argonne”). Argonne, a U.S. Department of Energy Office of Science laboratory, is operated under Contract No. DE-AC02-06CH11357. The U.S. Government retains for itself, and others acting on its behalf, a paid-up nonexclusive, irrevocable worldwide license in said article to reproduce, prepare derivative works, distribute copies to the public, and perform publicly and display publicly, by or on behalf of the Government. The Department of Energy will provide public access to these results of federally sponsored research in accordance with the DOE Public Access Plan <http://energy.gov/downloads/doe-public-access-plan>.